Studies on Effective Thermal Conductivities in Packed Beds

SAKAE YAGI and DAIZO KUNII

University of Tokyo, Tokyo, Japan

Applying both their own assumptions and the mechanism of lateral mixing proposed by Ranz (20), the authors obtained theoretical formulas for effective thermal conductivities k_e in packed beds. Previously reported experimental data were analyzed with these equations, and the usable data for prediction of k_e were shown.

In order to see the influence of both packing characteristics and temperature on the effective thermal conductivities, experimental data were obtained with air for beds with various kinds of packing, i.e., iron spheres, porcelain packings, cement clinker, insulating fire brick, and Raschig rings. Correlation of these data with Equation (15) showed that this equation adequately expressed the heat transfer mechanisms in packed beds with motionless gases, especially at high temperatures.

In the design of equipment for gas-solid reactions the proper values of the effective thermal conductivities must be estimated as simply as possible. On the basis of theoretical studies of heat transfer in these systems reported by Wilhelm (*22, 27*), Ranz (*20*), Damköhler (*7*), and Smith (*2*), the authors find that effective thermal conductivities can be separated into two terms, one of which is independent of fluid flow and the other dependent on the lateral mixing of the fluid in the packed beds. Thus theoretical equations of the effective conductivities in packed beds can be obtained that are simpler than equations previously reported. This paper reports four studies: first, the derivation of theoretical equations presented by Yagi and Kunii (*28*); second, an analysis of experimental data presented by several investigators; third, an outline of experiments on effective thermal conductivities in various kinds of packed beds with motionless air; and, fourth, an analysis of the experimental data by means of the authors' theoretical equations.

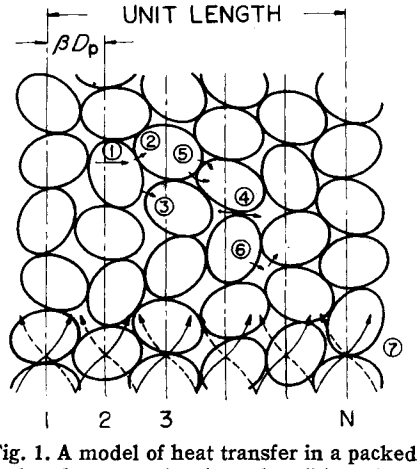

Fig. 1. A model of heat transfer in a packed bed. 1, heat transfer through solid; 2, heat transfer through the contact surface of solid; 3, radiant heat transfer between surfaces of solid (in case of gas); 4, radiant heat transfer between adjacent voids (in case of gas); 5, heat transfer through the fluid film near the contact surface; 6, heat transfer of convection, solid-fluid-solid; 7, heat transfer by lateral mixing of fluid, proposed by W. E. Ranz (20).

THEORETICAL EQUATIONS

Fundamental Assumptions

A model of heat transfer in packed beds is shown in Figure 1. Seven processes are discussed as follows:

Heat transfer mechanisms independent of fluid flow

1. Thermal conduction through solid
2. Thermal conduction through the contact surfaces of two packings
3. Radiant heat transfer between sur-

TABLE 1. ANALYTICAL RESULTS OF EXPERIMENTAL DATA OF EFFECTIVE THERMAL CONDUCTIVITIES IN PACKED BEDS WITH FLUID FLOW

$$k_e/k_g = k_e^\circ/k_g + (\alpha\beta)N_{pr}N_{ReM} = k_e^\circ/k_g + (\alpha\beta)N_{peM}$$
$$N_{ReM} = GD_p/\mu$$

Reference	Solid Gas	Diam. of solid, mm.	Diam. of bed, mm.	Data obtained N_{ReM}	k_e°/k_g	$(\alpha\beta)$	D_p/D_T
9	Catalyst cylinder Air	3.6 6.0 10.5	25.4 50 100	0∼ 1,000	5.5	0.10	0.036∼ 0.24
3	Alumina cylinder Air	3.18	51	0∼ 100	5.0	0.0833	0.0624
5	Celite cylinder Air	3.18 12.7	127	70∼ 3,500	10.4	0.136	0.025∼ 0.10
4	Silica-alumina, alumina, glass, cylinder, tablet, sphere Air, natural gas	4.9 25.4	51 102 153	0∼ 140	10.0	0.10	0.32∼ 0.37
	Glass, metal sphere Air, H_2, CO	2.46 7.42			—	0.090	0.246∼ 0.0742
1	Catalyst Air	10	100	0.1∼ 3,000	—	0.110	∼0.10
	Raschig ring Air	15×15			—	0.226	0.15
	Broken solid marble, etc. Air	2.85 16.5	52 154	30∼ 630	10	0.13	0.03∼ 0.17
15	Raschig ring (Fig. 7) Air	6.74 25	52 154	60∼ 650	3	0.24 0.17 0.12	0.10 0.15 0.20
	Berl saddle (Fig. 7) Air	12.5 25	100 154	70∼ 970	6	0.165 0.138 0.109	0.081 0.162 0.250
15	Catalyst cylinder annular space Air	3.6 6.0 10.5	154/48.5 100/34 154/27	20∼ 700	5.5	0.10	0.02∼ 0.105
21	Catalyst cylinder Air	3.18 4.76 6.36	50.8	0∼ 400	3.4 4.6 4.6	0.14 0.12 0.10	0.0625 0.0935 0.125
19	Glass sphere Air	13.3 18.2	205.0	100∼ 2,000	25.6	0.102	0.065 0.088
29	Iron sphere glass sphere insulating firebrick sphere, Air	11.0 6.0 10.0	52.9	50∼ 400	k_e°/k_g by Eq. (15)	0.12	0.114∼ 0.208

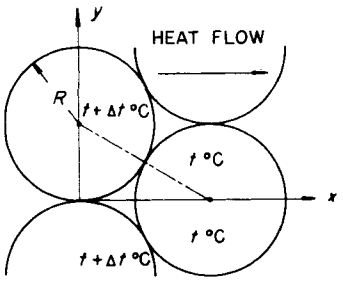

Fig. 2. Two-dimensional model of heat transfer through the fluid film in the void of packed bed.

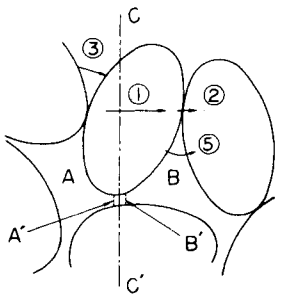

Fig. 3. A model of heat transfer without flowing fluid. A': black body surface representing void A; B': black body surface representing void B; CC': cross section perpendicular to the direction of heat flow.

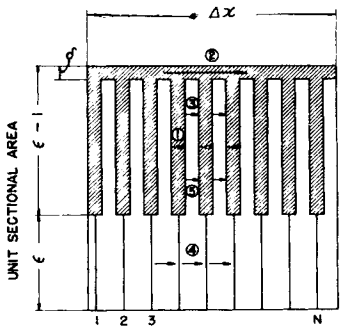

Fig. 4. Simplified model of heat transfer in packed bed without flowing fluid.

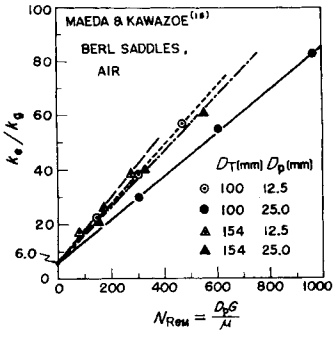

Fig. 5. Data for Berl saddles, by Maeda and Kawazoe (*15*).

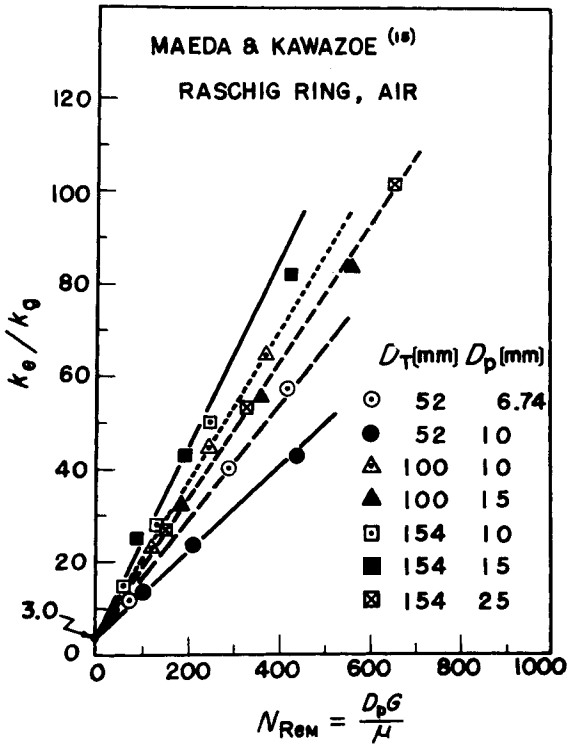

Fig. 6. Data for Raschig rings, by Maeda and Kawazoe (*15*).

faces of two packings (in the case of gas)

4. Radiant heat transfer between neighboring voids (in the case of gas)

Heat transfer mechanisms dependent on fluid flow

5. Thermal conduction through the fluid film near the contact surface of two packings
6. Heat transfer by convection, solid-fluid-solid
7. Heat transfer by lateral mixing of fluid

Mechanism 5 is calculated theoretically in the case of a two-dimensional model as shown in Figure 2, and it is found that nearly all the heat flows through the thin films of fluid near the contact point or surface of the two solids. Therefore it can be assumed that fluid flow has little effect on mechanism 5, because the fine interstices near the contact surfaces are embedded in the boundary layers except in the case of large Reynolds number.

When the Reynolds number is small, the boundary layers around the solid packings are thick; therefore mechanisms 1, 3, 4, and 5 are predominant. However, in the case of a large Reynolds number, process 7 controls the heat flux in any packed bed, and therefore the effect of mechanism 6 on the total rate of heat flow is slight. The theoretical equations containing mechanism 6, as well as the other processes, show that the effects of the convectional heat transfer mechanism solid-fluid-solid are small at all Reynolds numbers; the authors assume therefore that (1) thermal conduction through the thin film of fluid near the contact surfaces is not affected by fluid flow and (2) the convectional heat transfer mechanism solid-fluid-solid is less important than the other mechanisms and can be safely neglected.

Effect of Fluid Flow

Effective thermal conductivity caused by the lateral mixing of fluid is presented by Ranz (*20*) as the following equation:

$$(k_e)_t = \alpha C_p G/N \qquad (1)$$

The factor β is defined as the ratio of the average length l_p between the centers of two neighboring solids in the direction of heat flow to the mean diameter of packing D_p.

$$\beta = l_p/D_p \qquad (2)$$

In practical packed beds β takes a limited value between 0.82 and 1.0 for the wide ranges of packing characteristics. According to the definitions of both N and l_p,

$$N = 1/l_p = 1/\beta D_p \qquad (3)$$

From Equations (1) and (3),

$$(k_e)_t/k_g = (\alpha\beta)N_{pr}\cdot N_{ReM} = (\alpha\beta)N_{peM}$$

$$N_{pr} = C_p\mu/k_g,$$

$$N_{ReM} = D_pG/\mu, \qquad (4)$$

$$N_{peM} = D_pC_pG/k_g$$

The effective thermal conductivity, caused by the heat transfer mechanisms (1 to 5 in Figure 1) in the packed beds with motionless fluid, is defined by $k_e°$, a value that, according to assumptions 1 and 2 above, can be considered to remain constant and in parallel with the mechanism of lateral mixing when the fluid flows through the packed bed. Therefore, the effective thermal conductivity in packed beds is formulated as follows:

$$k_e = k_e° + (k_e)_t \qquad (5)$$

Applying Equation (4) gives

$$\frac{k_e}{k_g} = \frac{k_e^\circ}{k_g} + (\alpha\beta)N_{pr}N_{ReM}$$

$$= \frac{k_e^\circ}{k_g} + (\alpha\beta)N_{peM} \qquad (6)$$

Although the value of α is 0.179 in case of the rhombohedral packing of spheres (*20*), such values seem to change considerably in an actual packed bed according to the shape of the packings, the fraction void, and the ratio of the packing diameter to the bed diameter.

Motionless Fluids

In Figure 3 the heat transfer mechanisms in the series containing the thermal conduction in the solid phase arise in the fraction $(1 - \epsilon)$ of the sectional area $C - C'$ and then the radiant heat flows from one void to another through the fraction ϵ of the sectional area.

The heat transfer coefficient of thermal radiation can be formulated as the following equations, with the two parallel surfaces of black body A' and B' near the section $C - C'$ as shown in Figure 3 assumed to represent the two voids A and B respectively:

from solid surface to solid surface

$$h_{rs} = 0.1952\{p/(2 - p)\} \cdot \{(t + 273)/100\}^3 \qquad (7)$$

from void to void

$$h_{rv} = \left[0.1952 \Big/ \left\{1 + \frac{\epsilon}{2(1 - \epsilon)} \cdot \frac{1 - p}{p}\right\}\right]\{(t + 273)/100\}^3 \qquad (8)$$

Then the over-all heat transfer rate q [kcal./(sq. m.)(hr.)] is formulated as Equation (9) by application of a model of heat transfer in a packed bed with motionless fluid as shown in Figure 4.

$$q = \frac{k_e^\circ}{\Delta x}\Delta t = \delta\frac{k_s}{\Delta x}\Delta t + U_s(1 - \epsilon - \delta)\Delta t + V_v\epsilon\Delta t \qquad (9)$$

$$\frac{1}{U_s} = (N\Delta x)\left\{\frac{l_s}{k_s} + \frac{1}{k_g/l_v + h_{rs}}\right\} = (N\Delta x)\left\{\frac{\gamma D_p}{k_s} + \frac{1}{k_g/(\varphi D_p) + h_{rs}}\right\} \qquad (10)$$

$$\frac{1}{U_v} = N\Delta x\frac{1}{h_{rv}} \qquad (11)$$

where

γ = length of solid affected by thermal conductivity/mean diameter of solid = l_s/D_p

δ = total area of perfect contact surfaces as solid phase in sectional area of section $C - C'$/sectional area of section $C - C'$

φ = effective thickness of fluid film in void in relation to thermal conduction/mean diameter of solid = l_v/D_p (12)

The general equations are derived from Equations (9) through (12).

General equation

$$\frac{k_e^\circ}{k_g} = \delta\left(\frac{k_s}{k_g}\right) + \frac{(1 - \epsilon - \delta)\beta}{\gamma\left(\frac{k_g}{k_s}\right) + \frac{1}{\frac{1}{\varphi} + \frac{D_p h_{rs}}{k_g}}} + \epsilon\beta\frac{D_p h_{rv}}{k_g} \qquad (13)$$

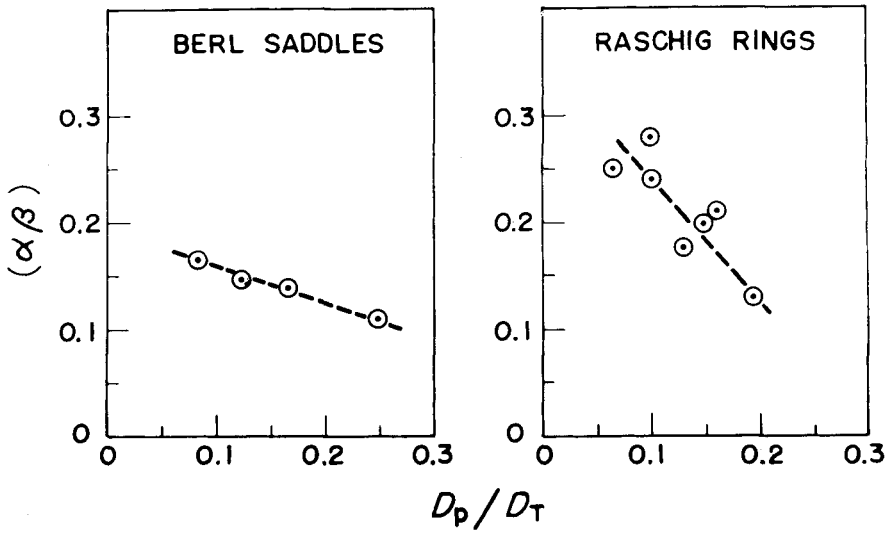

Fig. 7. Values of $(\alpha\beta)$ obtained from data by Maeda and Kawazoe (*15*).

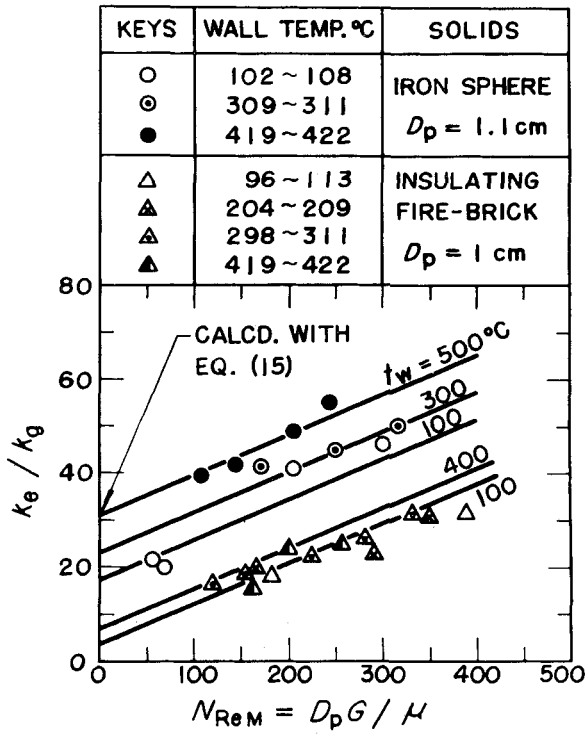

Fig. 8. Effects of wall temperature and thermal conductivities of solid particles on the effective thermal conductivities, by Yagi, Kunii and Shimomura (*29*).

Equations for special cases can be derived from Equation (13) as follows:

In vacuum

$$\frac{k_e^\circ}{k_s} = \delta + \frac{(1 - \epsilon)\beta}{1 + k_s/(D_p h_{rs})} + \epsilon\beta\frac{D_p h_{rv}}{k_s} \qquad (14)$$

In case of gas-filled voids

$$\frac{k_e^\circ}{k_g} = \frac{\beta(1 - \epsilon)}{\gamma\left(\frac{k_g}{k_s}\right) + \frac{1}{(1/\varphi) + (D_p h_{rs}/k_g)}} + \epsilon\beta\frac{D_p h_{rv}}{k_g} \qquad (15)$$

Table 2. Observers and Experimental Conditions in Figures 9 and 10.

Observer	Solid	Average diam.	Keys in Figures 9 and 10
Kling (*14*)	Steel sphere	3.8	(1)
Schuman and	Steel sphere	1.27	(2)
Voss (*24*)	Lead sphere	2.62	(2)
Waddems (*26*)	Steel sphere	1.59 ~ 7.94	(3)
Waddems (*26*)	Lead sphere	1.59 ~ 7.94	(4)
Waddems (*26*)	Steel cylinder, hexagonal prism		(5)
Kannuluick (*13*)	Carborundum	40 ~ 600	(6)
Schuman and Voss (*24*)	Quartz		(7)

In case of fine particles with motionless gas

$$\frac{k_e^\circ}{k_g} = \beta \frac{1-\epsilon}{\frac{k_g}{k_s} + \varphi} \qquad (16)$$

Equation (16) can be used for the packed bed of highly conductive solids with voids filled in with liquid. For practical purposes the values of both β and γ can be assumed as approximately unity.

ANALYSIS OF DATA PREVIOUSLY REPORTED WITH THEORETICAL EQUATIONS

Fundamental Data ($\alpha\beta$) for Beds with Fluid Flow

Experimental data previously reported concerning the effective thermal conductivities in packed beds with fluid flow can be separated into two groups:

1. k_e^∞, over-all thermal conductivities, the values of which incorporate the resistance to heat transfer within the bed, as well as at the walls of the confining tube (*10, 14, 16, 23, 25*).

2. k_e, the mean value in packed bed, the heat transfer resistance at the walls of the confining tube being removed (*1, 3, 4, 5, 8, 9, 15, 19, 21*).

According to the results of Hatta and Maeda (*9*), the value of k_e^∞ is about half that of k_e when $N_{ReM} = 800$; therefore the experimental data of k_e^∞ are omitted here.

When given experimental equations or data are transformed into standard form, i.e., Equation (6), the most important values of $(\alpha\beta)$ in packed beds can be obtained as summarized in Table 1. For example, some data by Maeda and Kawazoe (*15*) for Berl saddles and Raschig rings are shown in Figures 5 and 6 respectively, where the value of $(\alpha\beta)$ varies considerably with the ratio of solid diameter D_p to tube diameter D_T as shown in Figure 7. For spheres, cylinders, pellets, or broken granules the values of $(\alpha\beta)$ cover a narrow range, i.e., 0.1 to 0.14 for the different packing conditions. Since the Raschig ring has a hole through which the fluid may flow, the probability of lateral mixing in a bed packed with these rings can be assumed to be about twice that for ordinary solid packing.

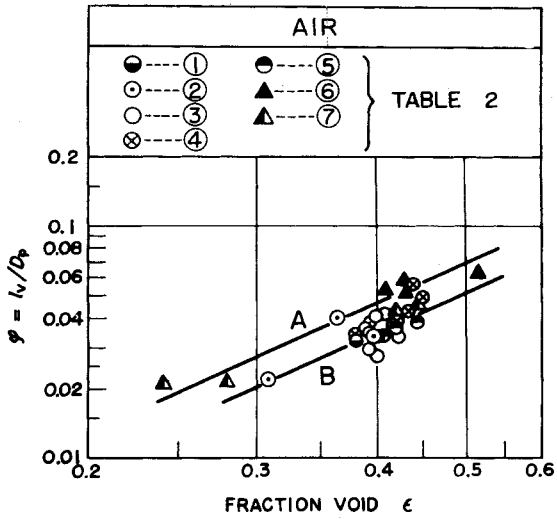

Fig. 9. Values of φ, calculated from experimental data previously reported (for air).

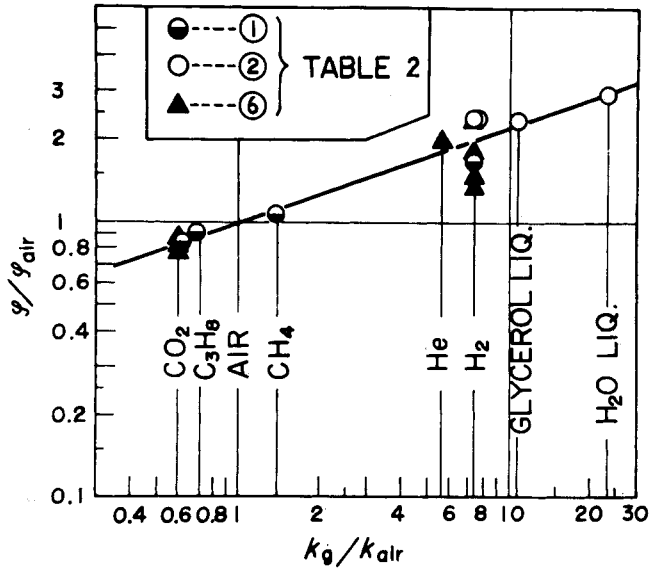

Fig. 10. Ratio (φ/φ_{air}) obtained from experimental data previously reported (for various kinds of fluid).

Being affected by the physical characteristics of solid packing, the values of k_e/k_g for iron spheres differ considerably from those for insulating fire bricks as shown in Figure 8, where the calculated values of k_e°/k_g derived with Equation (15) coincide fairly well with the experimental data obtained by the authors.

Effective Thermal Conductivities k_e° with Motionless Fluid

When experimental data for k_e° previously reported are analyzed by means of Equation (14) in packed beds of powdery materials, i.e., quartz, zinc, and iron, under reduced pressure of 0.05 to 0.20 mm. Hg, it is found that the values of δ are smaller than 10^{-5}. Therefore, it is reasonable to eliminate δ in Equation (13) under atmospheric pressure.

Analyzing the experimental data of k_e° reported by Kling (*14*), Schuman and Voss (*24*), Waddems (*26*), and Kannuluick (*13*) for solid packings of high thermal conductivities, i.e., steel, lead, Carborundum, and quartz, by means of Equation (15) or (16) yields the fundamental data of φ, shown in Figure 9 for air and in Figure 10 for the various fluids.

According to curve B for cylinders or spheres in Figure 9, the value of φ is 0.034 for the fraction void $\epsilon = 0.4$; then the effective thickness of fluid film in voids seems much smaller than the nominal length of the void, an indication of the importance of the thin film of fluid near the contact surfaces of two solids, as shown above.

Experimental data for effective thermal conductivities in a packed bed with motionless fluid, which the thermal conductivities of solids affect seriously, are compared with the calculated value by use of Equation (15), the values of φ being obtained from Figures 9 and 10 for the given values of fraction void ϵ. The results of this calculation are sum-

marized in Table 3, which indicates that theoretical equations (15) can correlate with the experimental data under different experimental conditions.

EXPERIMENTS

Apparatus

The experimental equipment (Figure 11) is similar to that used by other workers (*11, 12, 17*) for measurement of effective thermal conductivities in packed beds with motionless air. The column is constructed from a stainless steel tube with a Carborundum electric heater held in a coaxial silica tube. The solids are packed in the space between the two tubes, and the heat losses along the axis are obviated by the almost constant temperature distribution achieved by the adjustment of compensating electric heaters. Equally spaced chromel-alumel thermocouples are installed in the positions shown in Figure 11.

Procedure

Three to six hours after the electric heaters are switched on, heat flow attains steady state, and temperature, electric current, and voltage may be measured. Intervals between measurements under the same conditions are nearly 20 or 30 min. for all operating runs. The physical characteristics of the solid used for these experiments are shown in Table 4.

Experimental Results*

The values of effective thermal conductivities $k_e°$ in packed beds with motionless air are calculated by the following equations:

$$(0.860)VI = \frac{\pi l k_e° \Delta t}{2.3 \log_{10}(D_0/D_i)} \quad (17)$$

$$\Delta t = t_{B3} - t_{A3} \quad (18)$$

On application of the following values, Equation (19) is derived from Equation (17):

$$l = 0.25,\ D_0 = 0.146,\ D_i = 0.0375$$

$$k_e° = 0.743(VI)/\Delta t \quad (19)$$

Several examples of radial distribution of temperature are shown in Figure 12, where the distribution seems nearly straight; therefore, the mean temperature of the packed bed t_m, based on the volume of the solids, can be obtained easily. The ratio of $k_e°$ to the thermal conductivity of the air k_g is plotted with respect to the mean temperature of the packed bed t_m, as shown in Figures 13 to 17, where the following values of k_g are used for numerical calculations:

*Complete tabular material has been deposited as document 5305 with the American Documentation Institute, Photoduplication Service, Library of Congress, Washington 25, D. C., and may be obtained for $2.50 for photoprints or $1.75 for 35-mm. microfilm.

Table 3. Comparison of Calculated Values of $k_e°/k_g$ with Experimental Data Previously Reported

Reference	Solid	Fluid	Avg. Diam., D_p mm.	Exp. $k_e°/k_g$	Temp., °C.	Fraction void ϵ	k_s, kcal./(m.)(hr./°C.)	Calcd. $k_e°/k_g$
	Glass	He	—	2.60	10	0.35	0.60*	2.42
13	Glass	Air	—	6.62	10	0.35	0.60*	9.30
	Diphenylamine	H_2	—	1.00	10	0.513	0.189	0.48
	Diphenylamine	Air	—	3.30	10	0.513	0.189	2.68
24	Coal	Air	—	5.23	40*	0.437	0.60*	6.15
		H_2	—	1.53	40*	0.437	0.60*	1.46
	Catalyst	Air	3.6	5.40†	130	0.40	0.30*	5.48
9	cylinder	Air	6.0	5.98†	130	0.40	0.30*	5.98
		Air	10.5	6.20†	130	0.40	0.30*	6.00
14	Glass sphere	Air	4.06	12.0	60*	0.40	1.0*	11.0
3	Alumina pellet	Air	3.18	5.0†	300	0.40	0.30	5.04
		Air	0.64	9.8	140	0.39	1.6*	9.7
18	Sand	Air	0.13	9.8	140	0.37	1.6*	10.9
		Air	0.73	7.7	140	0.41	1.6*	8.95
	Hydrated alumina	Air	8	10†	50*	0.40*	0.92	11.3
4	alumina, sphere, pellet	Air	12		50*	0.40*	2.68	15.2
5	Celite	Air	3.18	11.4†	80*	0.40*	0.30*	5.5
	cylinder	Air	12.7				0.30*	8.0
15	Broken	Air	2.85	10†	140	0.45	2.2*	8.7
	solid	Air	16.5		140	0.45	2.2*	13.8

*Estimated values.
†Extrapolated values, $N_{Re_M} \to 0$.

t, °C.	0	200	400	600	800	1,000	1,200
k_g	0.0211	0.0338	0.0447	0.0534	0.0602	0.0655	0.0696

Data from Cowling (*6*).

Table 4. Characteristics of Solids Used for Experiments on Effective Thermal Conductivities with Motionless Air

Solid	Nominal diam., mm.	Fraction void ϵ	D_p, mm.	Data used for calculation of $k_e°/k_g$: k_s, kcal./(m.)(hr./°C.)	k_s/k_g	φ*	β	γ
Iron sphere	11.0	0.40	11.0	45 const.	—	0.034	1.0 and 0.9	1
Porcelain cylinder	9.6×8.5	0.43	9.05†	1.4 const.	—	0.040	1	1
Porcelain granule	6.0	0.43	6.0	1.4 const.	—	0.040	1	1
Cement clinker	5.0	0.50	5.0			0.050		
	3.6	0.50	3.6	1.7 const.	—	0.050	1	1
	2.6	0.50	2.6			0.050		
	0.35 ~ 0.01	0.54	0.18			0.060		
Insulating fire brick, cube	10	0.40	10.0	0.20 at 400°C.	4.48 const.	0.034	1	1
Insulating fire brick, sphere	5.0	0.50	5.0	0.20 at 400°C.	4.48 const.	0.050	1	1
Raschig ring								
Regularly packed	9 × 9 thickness	0.67	9.0	1.40 const.	—	0.034	$1/\sqrt{3}$	1.2/9
Randomly packed	1.2	0.72	9.0		—	0.034	$1 \times 1/3 + (1/\sqrt{3}) \times 2/3$	1.2/9

*The values of φ are obtained from B line in Figure 9.
†Mean value.

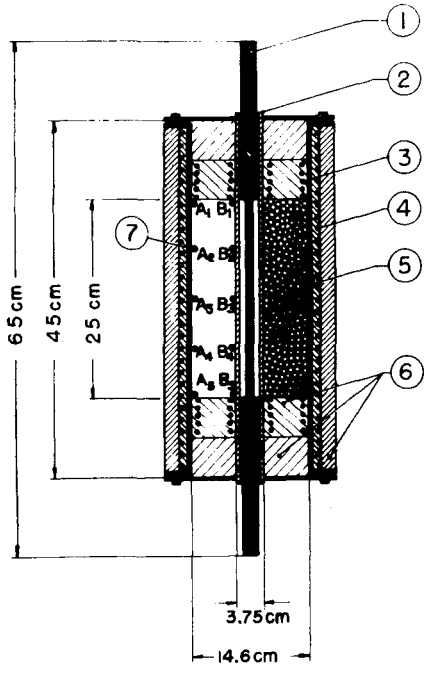

Fig. 11. Experimental packed bed with stagnant air, for measurement of effective thermal conductivities. 1, SiC electric heater; 2, silica tube; 3, Nichrome wire for compensation of lateral heat loss; 4, Nichrome wire for adjustment of bed temperature; 5, packed bed; 6, insulating fire brick; 7, position of thermocouples.

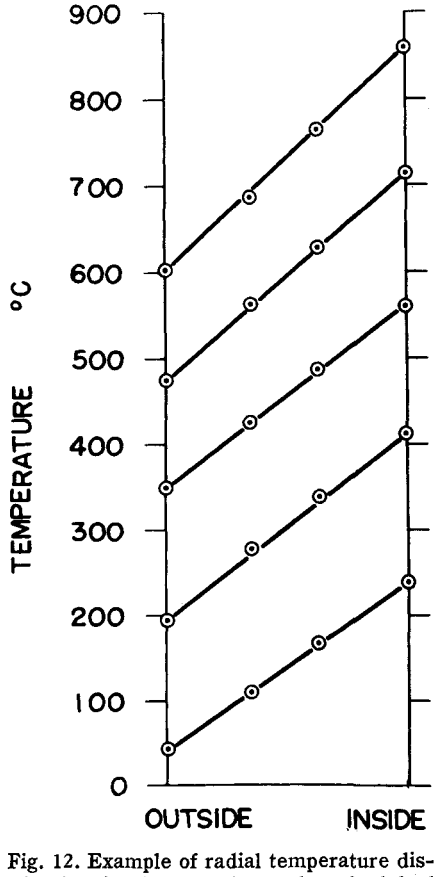

Fig. 12. Example of radial temperature distribution in the experimental packed bed without flowing fluid.

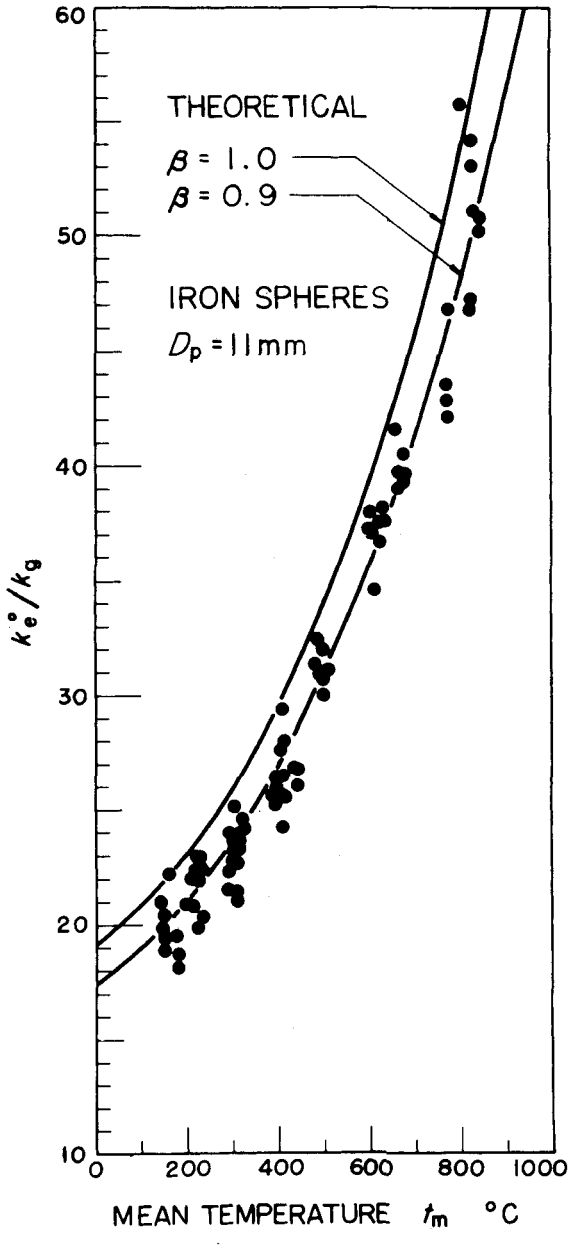

Fig. 13. Data obtained for packed beds of iron sphere, D_p = 11 mm.

Discussion

Since the values of $k_e°/k_g$ increase with the increase of the mean temperature of the packed bed t_m, radiant heat transfer seems to predominate when the mean temperature is high and the diameter and thermal conductivity of solids are large.

It is natural that the radiant heat transfer from solid to solid seriously affects the total heat flow in the case of iron spheres (Figure 13), because of the high conductivity of the solid phase. On the other hand, thermal radiation from void to void causes considerable heat flux even in the case of poorly conductive solids when the mean temperature of the packed bed is higher than 400°C., as shown in Figure 16.

The mean diameter of the solid greatly affects thermal conductivity, especially in the case of high temperature, as plotted in Figure 15, where the values of $k_e°/k_g$ are nearly constant for beds of particles smaller than 0.35 mm., an indication that thermal radiation can be neglected in such cases.

In Figure 17 the values of $k_e°/k_g$ for Raschig rings packed randomly are shown to be about 20% greater than those for rings packed regularly, because of the increase in the mean length of voids, which increases thermal radiation.

THEORETICAL VALUES COMPARED WITH EXPERIMENTAL DATA

In order to discuss the adequacy of the models of heat transfer mechanisms proposed by the authors, the theoretical

values of $k_e°/k_g$ are calculated from Equation (15) by taking the numerical values of the thermal conductivities of solid k_s and the factors β or γ as shown in Table 4 and comparing the results of calculation with the experimental data in Figures 13 to 17.

Although the equations derived by the authors are simple and contain some assumptions, they explain the experimental data fairly well, and the heat transfer models applied by the authors are sufficient to express the phenomena occurring in packed beds. Selection of the factors β, γ, and φ for beds packed with spheres, cylinders, or granules is easy, as shown in Table 4, but it is more difficult to select these values in the case of beds packed with Raschig rings. The thickness of the Raschig rings used in the experiment was l_s = 1.2 mm.

$$\gamma \doteqdot l_s/D_p$$

$$= 1.2 \text{ mm.}/9.0 \text{ mm.} = 0.0134$$

In beds packed regularly as shown in Figure 18, thermal radiation must pass through three voids in order to reach the point B from A or point B' from A'. Therefore, for the effective mean length of void l_p concerning the thermal radiation beam, the following value is assumed:

$$l_p = \sqrt{3}D_p/3 = D_p/\sqrt{3}$$

then

$$\beta = l_p/D_p = 1/\sqrt{3}$$

(regularly packed)

In the case of Raschig rings packed randomly, the possibility that the axis of the ring turns in the same direction as the heat flow is roughly considered as one-third, and so the value is assumed as

$$\beta = 1 \times (1/3) + (1/\sqrt{3}) \times (2/3)$$

Since the void spaces within the Raschig rings are fairly large, it can be considered that thermal radiation is superior to conduction through the air in the hollow spaces of the Raschig rings at temperatures above 300°C.; only the thin film of air between two rings effectively permits thermal conduction through the air. Therefore the value of φ selected is the same as for ordinary cylinders. The deviation of the experimental data from the calculated line in Figure 17 may be caused by the free convection in the wide spaces of the large fraction void ϵ = 0.67 to 0.72.

CONCLUSIONS

1. In the study of the mechanisms of heat transfer in packed beds with fluid flow and with motionless fluid in voids, several models of heat transfer mechanisms were applied and general equations of effective thermal conductivities in packed beds were obtained as Equations (6), (15), and (16).

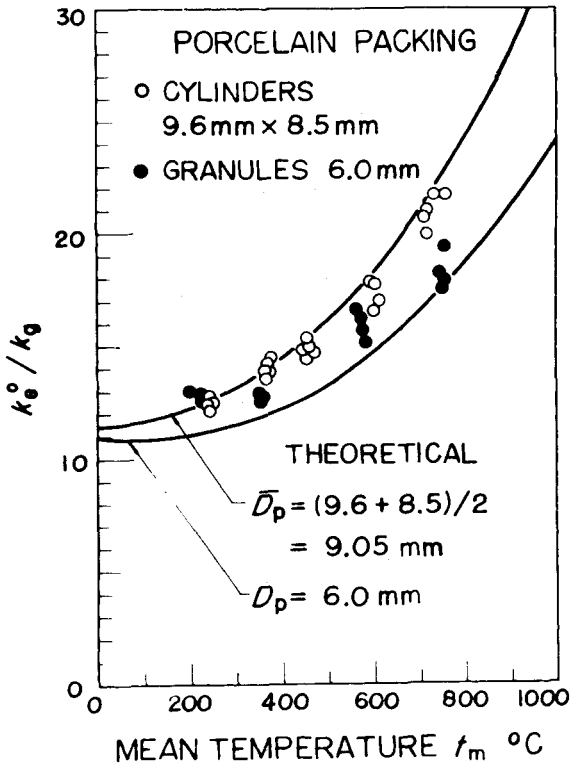

Fig. 14. Data for packed beds of porcelain packings.

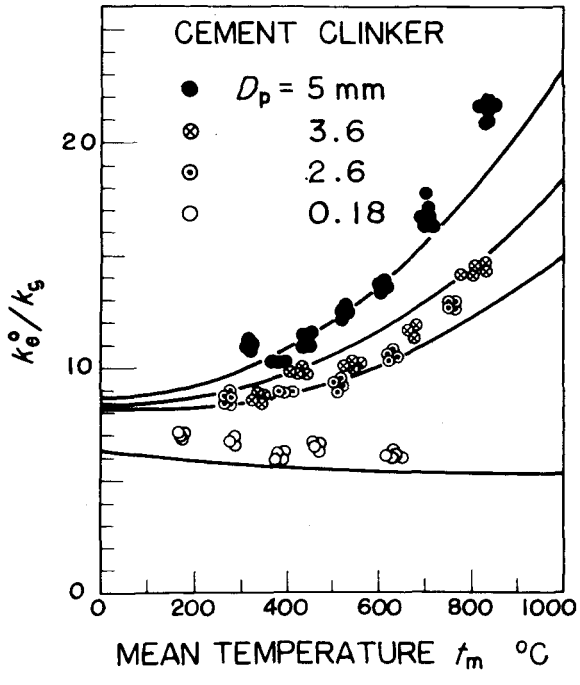

Fig. 15. Data for packed beds of cement clinker.

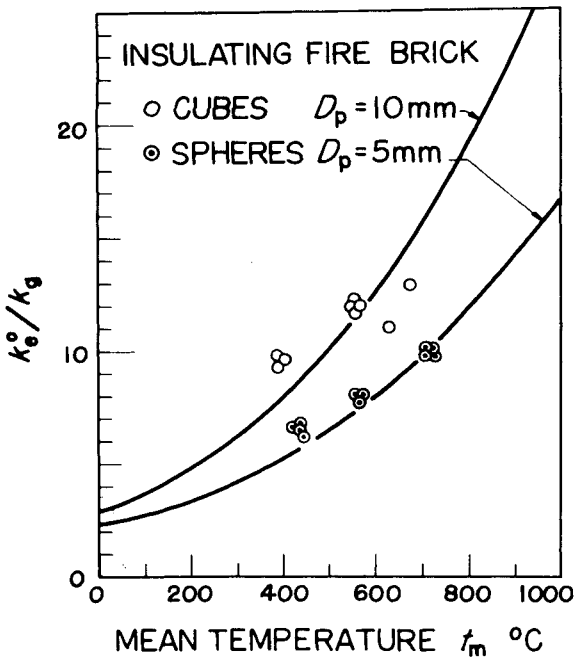

Fig. 16. Data for packed beds of insulating-fire-brick particles.

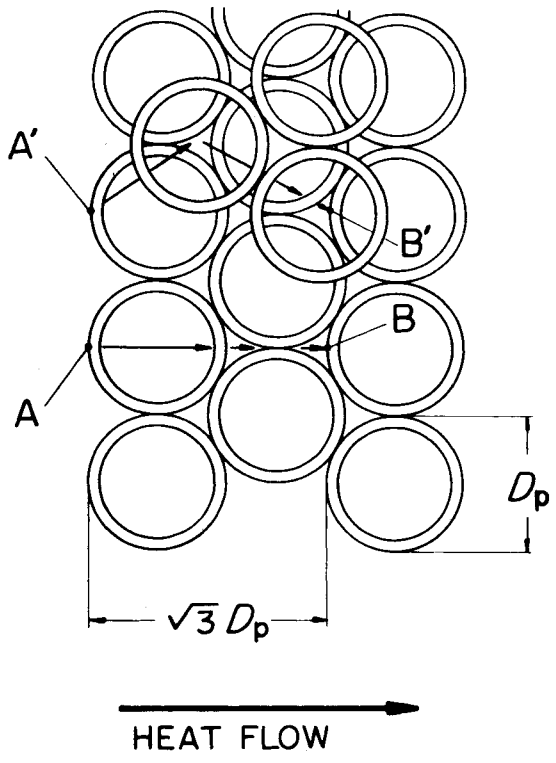

Fig. 18. Model of heat transfer in beds of Raschig rings packed regularly.

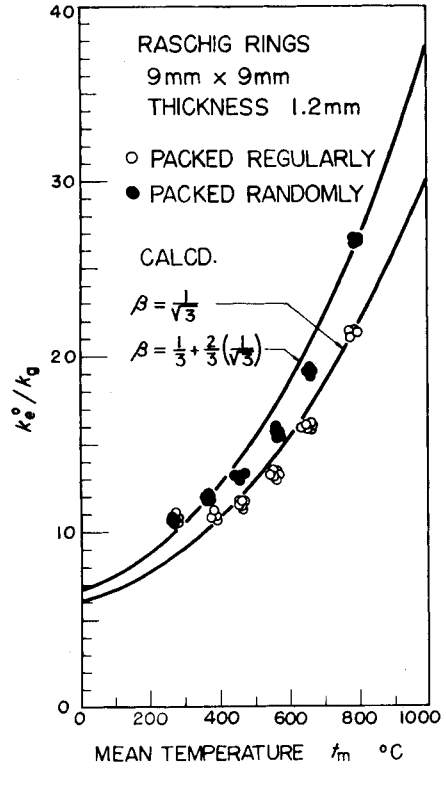

Fig. 17. Data for packed beds of Raschig rings.

2. Experimental data previously reported in cases of relatively low temperature were analyzed, and fundamental values for the calculation of the effective thermal conductivities by the authors' theoretical equations, i.e., α β and φ, were obtained as shown in Table 1 and Figures 7, 9, and 10.

3. Effective thermal conductivities in packed beds with motionless air were measured by collaborators of the authors for relatively high temperatures, and the radiant heat transfer mechanism was found to be most effective when the temperature of the bed was higher than 400°C. Both the diameters and the thermal conductivities of solid particles seriously affect the values of effective thermal conductivities in packed beds.

4. When results calculated from the authors' theoretical equation are compared with the experimental data presented, Equation (15) seems adequately to predict effective thermal conductivities in packed beds.

ACKNOWLEDGMENT

The authors wish to express their appreciation to Mitsuhiro Nakamura, Tomohiro Ito, and Shuichi Igarashi for their assistance in performing the experimental work.

NOTATION

C_p = specific heat of fluid, kcal./(kg.)(°C.)
D_p = nominal or average diameter of packing, m.
G = mass velocity of fluid, based on empty tube, kg./(sq. m.)(hr.)
I = electric current, amp.
h_{rs} = heat transfer coefficient for radiation, solid to solid, kcal./(sq. m.)(hr./°C.)
h_{rv} = heat transfer coefficient for radiation, void to void, kcal./(sq. m.)(hr./°C.)
k_e = effective thermal conductivity of packed bed with flowing fluid, kcal./(m.)(hr./°C.)
k_e° = effective thermal conductivity of packed bed with motionless fluid, kcal./(m.)(hr./°C.)
k_g = thermal conductivity of fluid, kcal./(m.)(hr./°C.)
k_s = thermal conductivity of packing material, kcal./(m.)(hr./°C.)
l = length of packed bed, m.
of two neighboring solids in the direction of heat flow, m.
l_p = effective length between the centers
l_s = effective length of solid relating to thermal conduction, m.
l_v = effective thickness of fluid film adjacent to contact surface of two solid particles, m.
N = number of solids in the unit length of packed bed, measured in the direction of heat flow
p = emissivity of solid surface
t = temperature, °C.
t_m = mean temperature of packed bed, °C.
V = voltage, volt

Greek Letters

α = mass velocity of fluid flowing in the direction of heat or mass transfer/

G = mass velocity of fluid based on sectional area of empty tube in the direction of fluid flowing
$\beta = l_p/D_p$
$\gamma = l_s/D_p$
$\varphi = l_v/D_p$
ϵ = fraction void

LITERATURE CITED

1. Aerov, M. E., and N. N. Umnik, *J. Appl. Chem. (U.S.S.R.)*, **27**, No. 3, 265 (1954).
2. Argo, W. E., and J. M. Smith, *Chem. Eng. Progr.*, **49**, 443 (1953).
3. Bunnell, D. G., H. B. Irvin, R. W. Olson, and J. M. Smith, *Ind. Eng. Chem.*, **41**, 1977 (1949).
4. Campbell, J. M., and R. L. Huntington, *Petroleum Refiner*, **30**, 127 (1951); **31**, 123 (1952).
5. Coberly, C. A., and W. R. Marshall, Jr., *Chem. Eng. Progr.*, **47**, 141 (1951).
6. Cowling, C., "Mathematical Theory of Non-Uniform Gases," Cambridge University Press (1952).
7. Damköhler, G., "Der Chemie Ingenieur 'Eucken Jakob,' " Vol. 3, Part 1, 441.
8. Felix, J. R., and W. K. Neill, Paper presented at A.I.Ch.E. Atlantic City meeting (1951).
9. Hatta, S., and S. Maeda, *Chem. Eng. (Japan)*, **12**, 56 (1948); **13**, 79 (1949).
10. Hougen, J. O., and E. L. Piret, *Chem. Eng. Progr.*, **47**, 287 (1951).
11. Igarashi, S., B.S. thesis, Univ. Tokyo (1956).
12. Ito, T., B.S. thesis, Univ. Tokyo (1955).
13. Kannuluick, W. G., and L. H. Martin, *Proc. Roy. Soc. (London)*, **A141**, 144 (1933).
14. Kling, G., *Forsch. Gebiete Ingenieuerw.*, **9**, 82 (1938).
15. Maeda, S., and K. Kawazoe, *Chem. Eng. (Japan)*, **15**, 5, 9, 312 (1951); **17**, 276 (1953); **18**, 279 (1954).
16. Molino, D. F., and J. O. Hougen, *Chem. Eng. Progr.*, **48**, 147 (1952).
17. Nakamura, M., B.S. thesis, Univ. Tokyo (1954).
18. Okada, S., and R. Toyabe, B.S. thesis, Univ. Tokyo (1953, 1954).
19. Plautz, D. A., and H. F. Johnstone, *J. Am. Inst. Chem. Engrs.*, **1**, No. 2, 193 (1955).
20. Ranz, W. E., *Chem. Eng. Progr.*, **48**, 247 (1952).
21. Schuler, R. W., V. P. Stallings, and J. M. Smith, *Chem. Eng. Progr. Symposium Ser.* No. 4, **48**, 19 (1952).
22. Singer, E., and R. H. Wilhelm, *Chem. Eng. Progr.*, **46**, 343 (1950).
23. Sugawara, W., and S. Sato, *Trans. Soc. Mech. Engr. (Japan)*, **13**, No. 45, 164 (1947).
24. Schuman, T. E. W., and V. Voss, *Fuel*, **13**, 249 (1934).
25. Verschoor, H., and G. Schuit, *Appl. Sci. Research*, **42**, A2, No. 2, 97 (1950).
26. Waddems, A. L., *J. Soc. Chem. Ind.*, **63**, 337 (1944); *Chemistry & Industry*, 206 (1944).
27. Wilhelm, R. H., W. C. Wynkoop, and D. W. Collier, *Chem. Eng. Progr.*, **44**, 105 (1948).
28. Yagi, S., and D. Kunii, *Chem. Eng. (Japan)*, **18**, 576 (1954).
29. Yagi, S., D. Kunii, and Y. Shimomura, *Chem. Eng. (Japan)*, **21**, 342 (1957).

Behavior of Suspended Particles in a Turbulent Fluid

S. K. FRIEDLANDER

Columbia University, New York, New York

Heat and mass transfer and coagulation are considered as related to the mean-square relative velocity between particle and fluid $\overline{u_R^2}$ and eddy diffusion as described by the mean-square particle displacement, $\overline{X_P^2}$. The mathematical methods used are similar to those employed in the early calculations of the Brownian motion.

The mean-square relative velocity is obtained as a function of particle characteristics, intensity of turbulence, and a fluid correlation coefficient. In the limiting case of equal particle and fluid density $\overline{u_R^2} = 0$, and for very heavy particles $\overline{u_R^2} \rightarrow \overline{u_F^2}$.

A general expression for the eddy diffusivity is obtained which reduces to the same form as that of the fluid for the stationary state. However, the correlation coefficient to be used in the calculations depends on $\overline{u_R^2}$. As a first approximation, it can be assumed that at a sufficiently long time from the introduction of the particles, fluid and particle diffusivities are equal.

For short times after injection, the particle spread may be much less than that of the fluid. An illustrative calculation for the initial spreading of a jet of suspended particles is offered. In all cases an effort is made to organize the available experimental data within the framework of the theory.

The behavior of dilute suspensions of small particles in a turbulent fluid is of interest in agitation, fuel injection, erosion, silt transport, and cloud formation. During these processes a number of related effects may occur including (1) heat and mass transfer to the suspended particles, (2) eddy diffusion of the dispersed material, and (3) coagulation or collision.

Practically all the available experimental data are concerned with the second effect, eddy diffusion. The com-

S. K. Friedlander is now at The Johns Hopkins University, Baltimore, Maryland.